NUMERICAL ANALYSIS OF FLOW PATTERN AND MORPHOLOGICAL CHANGES IN TIDAL REACH OF SANGU RIVER, BANGLADESH

TABASSUM Khoshnoor [*]
MEE23724

Supervisor: Professor EGASHIRA Shinji [**]
Assoc. Professor HARADA Daisuke [***]
Prof. KATAYAMA Koji [****]

ABSTRACT

The Sangu River experiences significant riverbank erosion each year, driven by seasonal flood discharges and tidal currents from the Bay of Bengal. This erosion results in the shifting of the bank line, the migration of settlements, and threats to agriculture and vital infrastructure. This study aimed to investigate the effects of sediment transport, accelerated by high-velocity flows, on the river's morphological changes, particularly in the downstream section, and to assess the impact of proposed countermeasures to reduce riverbank erosion. A 2-D depth-averaged model for flow and bed deformation was applied to evaluate these morphological changes and calculate the extent of riverbank erosion and deposition. The results from numerical computations suggest that spiral currents at meandering bends, driven by accelerated river flow during flash floods and tidal events, are significant contributors to riverbank erosion. Elevated shear stress during neap tides leads to significant erosion, which can be exacerbated by flood discharge. Implementing countermeasures that reduce the flow path has been found to be effective in decreasing flow strength and, consequently, reducing riverbank erosion in affected areas. This study provides valuable insights that may assist policymakers in developing effective strategies for flood management and riverbank erosion control, contributing to sustainable development in the region.

Keywords: Sangu River, Morphological Changes, Riverbank Erosion, iRIC, Sediment Transportation.

INTRODUCTION

Riverbank erosion is a major issue in Bangladesh, causing loss of floodplain area, decreased agricultural productivity, and displacement of people, which worsens poverty. During the monsoon, large volumes of sediment from upstream areas contribute to flooding and erosion in meandering and braided rivers. Managing flow volume and predicting channel changes in these dynamic systems is challenging. The Delta Plan 2100 by the Government of Bangladesh aims to address water management and climate change, identifying the Sangu River Basin in the Chittagong Hill Tracts (CHT) as a key hotspot.

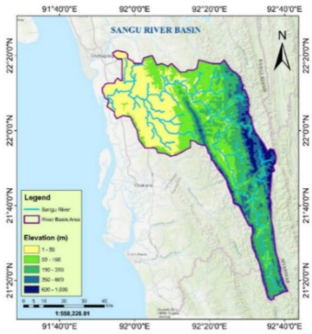

Figure 1. Study area (Sangu River basin)

The Sangu River, originating in Myanmar's North Arakan Hills and flowing into the Bay of Bengal, spans 270 km, with 173 km in Bangladesh. It faces challenges from flooding and riverbank erosion due to heavy monsoon sediment flows, which reduce depth and increase flood risk. This study analyzes how

---

[*]Sub-Divisional Engineer (C.C.), Bangladesh Water Development Board (BWDB), Bangladesh.
[**]Research and Training Advisor, Water-related Hazard Research Group, International Centre for Water Hazard and Risk Management, (ICHARM), PWRI, Japan.
[***]Research Specialist, Water-related Hazard Research Group, International Centre for Water Hazard and Risk Management, (ICHARM), PWRI, Japan.
[****]Director, Disaster Management Policy Program, National Graduate Institute for Policy Studies (GRIPS), Japan.

flood and tidal currents affect river morphology, predicts erosion-prone areas, and assesses intervention impacts to guide effective measures for protecting settlements and agricultural lands.

THEORY AND METHODOLOGY

The governing equations employed in the numerical model include mass and momentum conservation equations for water flow, along with mass conservation equations for suspended and bed sediment. These equations are complemented by a bed-load formula and erosion-deposition formulas for suspended sediment. The mass conservation equation (continuity equation) for water flow is as follows:

$$\frac{\partial \mathrm{h}}{\partial t}+\frac{\partial}{\partial x}(uh)+\frac{\partial \mathrm{h}}{\partial y}(vh)=0 \tag{1}$$

The momentum conservation equations for water flow are:

X-component: $$\frac{\partial u\mathrm{h}}{\partial t}+\frac{\partial uuh}{\partial x}+\frac{\partial uv\mathrm{h}}{\partial y}=-gh\frac{\partial}{\partial x}(h+z_b)-\frac{\tau_{\mathrm{x}}}{\rho}+\frac{1}{\rho}\{\frac{\partial}{\partial x}(h\tau_{\mathrm{xx}})+\frac{\partial}{\partial y}\ (h\tau_{\mathrm{yx}})\} \tag{2}$$

Y-component: $$\frac{\partial v\mathrm{h}}{\partial t}+\frac{\partial vuh}{\partial x}+\frac{\partial vv\mathrm{h}}{\partial y}=-gh\frac{\partial}{\partial y}(h+z_b)-\frac{\tau_{\mathrm{y}}}{\rho}+\frac{1}{\rho}\{\frac{\partial}{\partial y}\left(h\tau_{\mathrm{yy}}\right)+\frac{\partial}{\partial x}\ (h\tau_{\mathrm{xy}})\} \tag{3}$$

The mass conservation equation for suspended sediment is:

$$\frac{\partial c_i\,\mathrm{h}}{\partial t}+\frac{\partial \mathrm{r}_1\overline{c_l}\overline{u}h}{\partial x}+\frac{\partial \mathrm{r}_1\overline{c_l}\overline{v}\mathrm{h}}{\partial y}=\frac{\partial}{\partial x}\left(h\varepsilon_{\mathrm{x}}\frac{\partial\overline{c_l}}{\partial x}\right)+\frac{\partial}{\partial x}\left(h\varepsilon_{\mathrm{y}}\frac{\partial\overline{c_l}}{\partial y}\right)+E_i-D_i \tag{4}$$

Here, u and v are the velocity components in the x and y directions, respectively; h is the depth of flow; τ_{x} and τ_{x} are the x and y components of the bed shear stress (τ_{b}); $\mathrm{z_b}$ represents the bed elevation; τ_{xx}, τ_{yx}, τ_{yy}, and τ_{xy} are the Reynolds stresses; ε_{x} and ε_{y} are the x and y components of the dispersion coefficient (analogous to the turbulent diffusion coefficient). *Ei* and *Di* denote the erosion and deposition rates of sediment for grain size *di;* r_1 is the correction factor; $\frac{\partial z_b}{\partial t}$ represents the average bed variation.

The riverbed deformation $\frac{z_b}{\partial t}$ is evaluated as follows:

$$\frac{z_b}{\partial t}+\frac{1}{1-\lambda}\sum_i\left(\frac{\partial \mathrm{q_{bix}}}{\partial x}+\frac{\partial \mathrm{q_{biy}}}{\partial y}+E_i-D_i\right)=0 \tag{5}$$

Where $\mathrm{q_{bix}}$ and $\mathrm{q_{biy}}$ are the bed load transport rates in the x and y directions of the bedload transport rate for the sediment size class i (for grain size d_i); and λ is the porosity of bed sediment. These components are calculated using the formula proposed by Egashira et al. (1997) in this study.

The bed load formula (Egashira et al., 1997) is expressed as follows:

$$q_{b^*}=\frac{4}{15}\frac{K_1K_2}{\sqrt{f_d+f_f}}\ \tau_*^{\frac{5}{2}} \tag{6}$$

$$\tau_*=\frac{{u_*}^2}{\left(\frac{\sigma}{\rho}-1\right)gd} \tag{7}$$

$$u_*=\sqrt{ghsin\theta} \tag{8}$$

Here non-dimensional bed load transport rate is q_{b^*}, $\tau_*$is the non-dimensional bed shear stress, K_1, K_2, f_d and f_f are specified theoretically, d is the grain size, h is the flow depth and θ is the bed slope.

The rate of erosion of suspended sediment was evaluated using the entrainment velocity concept proposed by Harada et al. (2019):

$$E_i=p_iW_e\bar{c}_s \tag{9}$$

Where W_e represents the entrainment velocity at the boundary between the upper water layer and bedload layer, and $\bar{c}_s$ is the sediment concentration within the bedload layer. The entrainment velocity (*We*) was evaluated by using the following formula for a density-stratified flow:

$$\frac{W_e}{V}=\frac{K}{R_{i*}} \tag{10}$$

$$R_{i*}=\left(\frac{\sigma}{\rho}-1\right)\bar{c}_sgh/V \tag{11}$$

Where R_{i*} is the overall Richardson number and K = 1.5 × 10^{-3}, $\Delta\rho$ is the density difference between the water layer and bed load layer, V is the depth averaged velocity defined as V=$\sqrt{u^2+v^2}$.

The deposition rate was evaluated as follows:

$$D_i=w_{oi}c_i \tag{12}$$

where w_{oi} is the fall velocity of sediment particle size class i.

Computational Conditions

The computational domain for this study was established using the Nays2DH solver within the iRIC software, proposed by Takebayashi (2009) for modeling river flow, sediment transport, and morpho-dynamics which was used to simulate a channel 30 km stretch of the river's lower reach. The grid of the channel was extended beyond the left riverbank near the loop, as shown in Figure 3.4. The simulation conditions included a computational domain covering a 30 km length of the river, with the width varying from 400 m to 3,000 m. The grid size used was I=300×J=27=8,100 cells. The calculation time step was set to 0.25 seconds. Upstream discharge was considered as non-uniform flow, with a uniform sediment type. Manning's roughness coefficient was set at 0.03, and the sediment particle size was 0.3 mm.

DATA

Bathymetric surveys of the elevation of the riverbed surface conducted in 2018 by the Bangladesh Water Development Board (BWDB) field office were used to determine initial bed topography. The model domain extended from the river mouth to 7 km into the Bay of Bengal and 23 km upstream. An artificial bay was created to allow fluctuations and a buffer zone to allow tides.

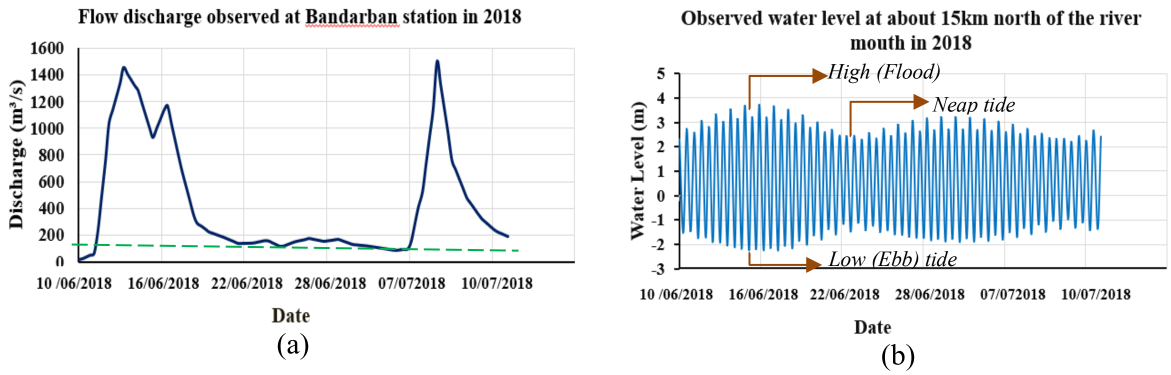

Figure 2. Flow discharge observed at Bandarban station in 2018 and (b) Observed water level at about 15Km north of river mouth in 2018.

Two boundary conditions were defined for the river:

- The upstream boundary condition was based on 30 days of monsoon flood data, collected by BWDB field office from June 10th to July 9th, 2018.
- For the downstream boundary condition tidal current from Bay of Bengal was considered. However, due to the absence of observational data for the tidal flow, a probable tidal water level was generated and applied in the model (Rahman, Harada, & Egashira, 2023). This generated tidal water level served as the downstream boundary condition in the study.

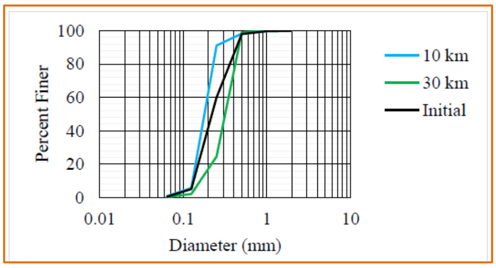

Figure 3. Initial size distribution of sediment particle of bed materials

RESULTS AND DISCUSSION

To check the accuracy of the tidal data used in the model, it was compared with the observed tidal water level from the available gauge station in Banigram, located downstream of the river which is shown in Figure 4. The simulated water levels agreed well with field data obtained from the gauge station. Rahman et.al. (2022) suggests local-scale analysis is necessary to understand channel-shifting mechanisms and propose countermeasures. Three cases have been conducted for the simulation described as follows. A 30-day simulation with a steady peak flood discharge of approximately 1,500 m^3/s was conducted.

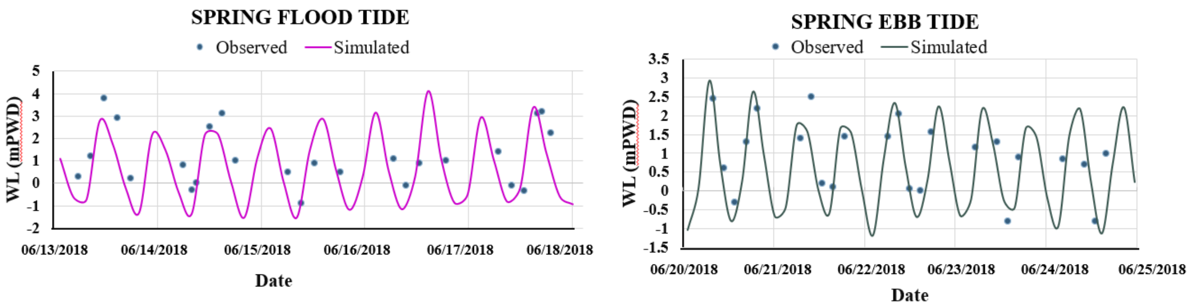

(a) (b)

Figure 4. Comparison of simulated water level with observed tidal water level (a) for a spring tide and (b) for a neap tide at station nearby downstream.

Case 1: Combination of flood discharge and tidal effect

A 30 days of non-uniform flow flood discharge with maximum observed discharge about 1500m^3/s from upstream region of the river has been considered along with tidal flow at the downstream as boundary condition to understand the combined effect of them on the river morphology. Bed deformation in rivers is heavily influenced by water flow dynamics, particularly at meandering bends where flow interacts with the riverbank curvature, creating high shear stress areas due to circular patterns like eddies. Numerical simulations show that shear stress, measured by the Shields number, peaks during low tide (ebb tide) of a spring tide, leading to maximum bed deformation (erosion) during this period. This effect is visually depicted in Figure 6, highlighting significant erosion downstream driven by tidal and flood currents.

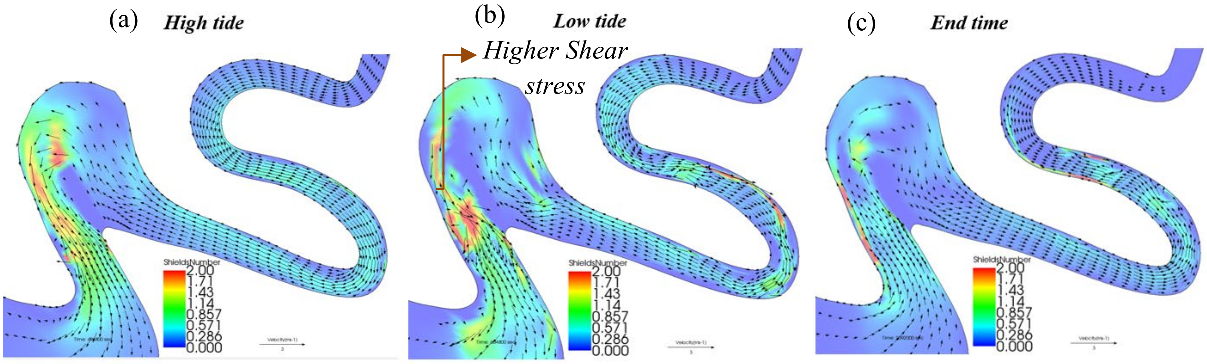

Figure 5. Shear stress profile in Case 1 (a) during high tide, (b) during low tide and (c) at end of computation.

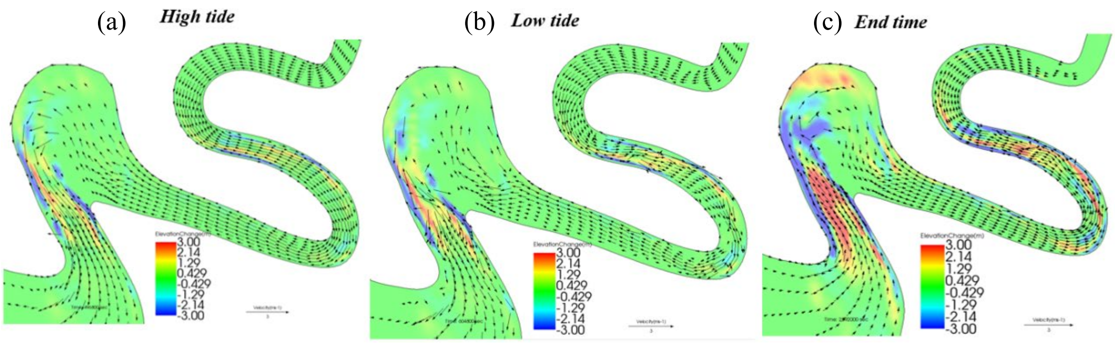

Figure 6. Bed deformation profile in Case 1 (a) during high tide, (b) during low tide and (c) at end of (after 30 days) computation.

Case 2: Tidal effect

In this case, a steady uniform flow discharge of 130m^3/s from upstream as upstream boundary condition and 30 days tidal current data at the downstream region of the river as downstream boundary condition has been considered to understand the effect of only tidal current from downstream on the river morphology. Comparison between shear stress and bed deformation profiles for Case 1 and Case 2 suggests that more active bed deformation in the downstream area occurs in presence of river during low tides part, particularly when flood flow coincides with tidal currents. Case 1 generates greater shear stress than in Case 2, where only tidal effects were considered, leading to increased erosion during low tide.

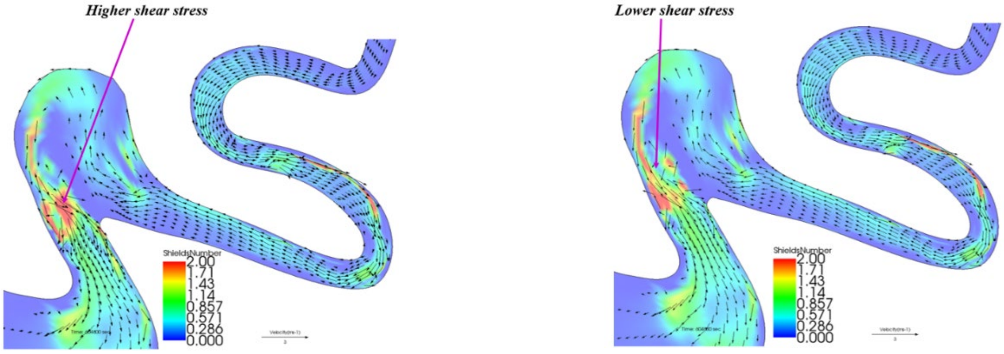

Case 1: Effect of seasonal flood flow & tidal flow   Case 2: Effect of tidal flow

Figure 7. Comparison of shear stress profile between Case 1 and Case 2 during low tide riverbank.

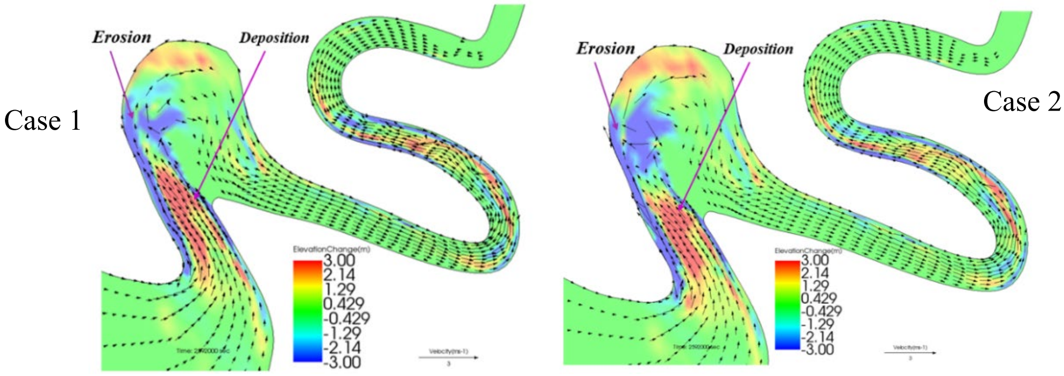

Figure 8. Comparison of shear stress profile between Case 1 and Case 2 during low tide riverbank

Case 3: Application of Countermeasure

The purpose of this intervention is to create a bypass that shortens the length of the existing river loop and divert the flow to reduce the flow strength, thereby preventing bed deformation. The expected benefits of this intervention include reduced erosion at the outer bend, a steeper water slope leading to increased flow velocity and decreased drainage congestion, and reduced sedimentation in downstream area of the river. Figure 9 shows that at the end of simulation less deposition and erosion occur along the right bank of the river where the river meets the Bay of Bengal.

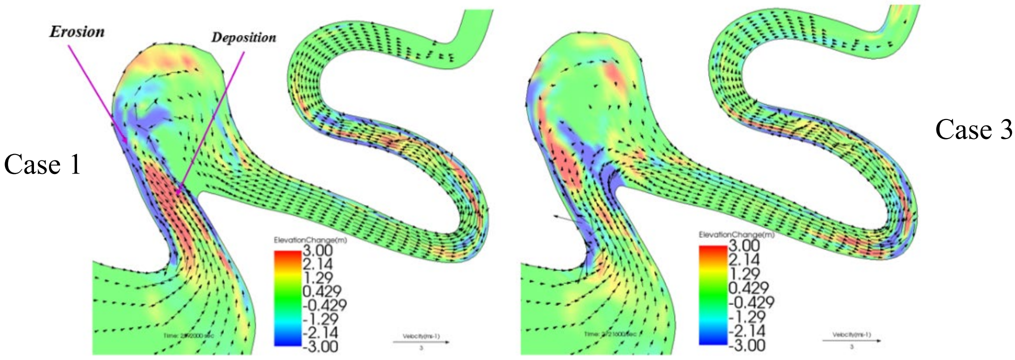

Figure 9. Comparison of bed deformation profile between Case 1 and Case 3 after 30 days of numerical computation

CONCLUSION AND RECOMMENDATION

The study finds that erosion occurs during the ebb (low) tide of spring tides, where shear stress is high, while sediment deposition happens during the high tide of spring tides when shear stress is low. Numerical computations reveal that spiral currents at meandering bends, intensified by accelerated river flow during flash floods and tidal events, are significant contributors to riverbank erosion. Elevated shear stress during neap tides can be exacerbated by flood discharge in downstream areas with large curvature.

Simulation results indicate that the proposed countermeasure reduces shear stress at bends compared to conditions without the countermeasure. However, further research should account for seasonal flow variations over multiple years and consider discharge scenarios for a 100-year return period. Future studies should also incorporate non-uniform bed materials and varying roughness conditions to better reflect actual field conditions. Additionally, dredging in strategic locations to enhance river capacity and drainage could be explored as a countermeasure. This study highlights the need for policy recommendations to address riverbank erosion in the Sangu River Basin.

ACKNOWLEDGEMENTS

I would like to thank my supervisors, Professor Dr. Shinji Egashira and Assoc. Professor Dr. Daisuke Harada, for their invaluable guidance, comments, and motivation throughout this study. I also extend my gratitude to Dr. Kattia Rubi Arnez Ferrel and Mr. Md. Shahinur Rahman for their continuous support.

REFERENCES

Egashira, S. and Ashida, K., 1980. Studies on the Structures of Density Stratified flows. Bulletin of the Disaster Prevention Research Institute, 29(4), pp.165-198.

Egashira, S. 2015. Mechanics of Sediment transportation and channel changes, Lectures notes, International Center for Water Hazard and Risk Management (ICHARM). Tsukuba: Public Works Research Institute (PWRI).

Harada, D., Egashira, S., Ahmed, T., & Ito, H. (2022). Entrainment of bed sediment composed of very fine material. Earth Surface Processes and Landforms, 1 11.

Rahman, M.M., Harada, D. and Egashira, S., 2024. Numerical Simulation of River Channel Change in the Suspended Sediment-Dominated Downstream Reach of the Sangu River. Water, 16(13), p.1934.

Rahman, M.M., 2023. Study on sediment runoff and morphological changes in the Sangu River basin, Bangladesh. ICHARM, GRIPS, Japan.